PROTEINS
STRUCTURE ■ FUNCTION ■ BIOINFORMATICS

Structural and functional studies of the potent anti-HIV chemokine variant P2-RANTES

Hongjun Jin,[1] Ioannis Kagiampakis,[1] Pingwei Li,[1] and Patricia J. LiWang[2]*

[1] Department of Biochemistry and Biophysics, Texas A&M University, College Station, Texas 77843-2128

[2] University of California Merced, School of Natural Sciences, Merced, California 95343

ABSTRACT

The N-terminal region of the chemokine RANTES is critical for its function. A synthesized N-terminally modified analog of RANTES, P2-RANTES, was discovered using a phage display selection against living CCR5-expressing cells, and has been reported to inhibit HIV-1 env-mediated cell–cell fusion at subnanomolar levels (Hartley et al. J Virol 2003;77:6637–6644). In the present study we produced this protein using *E. coli* overexpression and extensively studied its structure and function. The x-ray crystal structure of P2-RANTES was solved and refined at 1.7 Å resolution. This protein was found to be predominantly a monomer in solution by analytical ultracentrifugation, but a tetramer in the crystal. In studies of glycosaminoglycan binding, P2-RANTES was found to be significantly less able to bind heparin than wild type RANTES. We also tested this protein for receptor internalization where it was shown to be functional, in cell–cell fusion assays where recombinant P2-RANTES was a potent fusion inhibitor (IC_{50} = 2.4 ± 0.8 n*M*), and in single round infection assays where P2-RANTES inhibited at subnanomolar levels. Further, in a modified fusion assay designed to test specificity of inhibition, P2-RANTES was also highly effective, with a 65-fold improvement over the fusion inhibitor C37, which is closely related to the clinically approved inhibitor T-20. These studies provide detailed structural and functional information for this novel N-terminally modified chemokine mutant. This information will be very useful in the development of more potent anti-HIV agents. PDB Accession Number: 2vxw.

Proteins 2010; 78:295–308.

Key words: HIV fusion inhibitor; chemokine; GAG binding; quaternary state; competition fusion assay.

INTRODUCTION

Chemokines bind to seven transmembrane G-protein-coupled receptors (GPCRs) and mediate leukocyte activation and migration that is involved in a wide range of physiological phenomena including immunodefense, inflammation, wound healing and cancer development.[1–5] The CC chemokine, CCL5/RANTES (regulated upon activation normal T cell expressed and secreted) can bind and activate the chemokine receptors CCR1, CCR3, CCR4, and CCR5.[1,3,4] RANTES can consequently mediate activation and chemotaxis of macrophages (or monocytes), eosinophils, basophils, and T cells.[5,6] Due to its ability to mobilize these cell types, increased RANTES expression is related to a wide range of inflammatory disorders and pathologies. Importantly, RANTES also inhibits HIV entry and infection by competing with the virus for CCR5 binding, and as such has been a target for anti-HIV drug design.[1,7–11]

Mutagenesis experiments have supported the hypothesis that the N-terminal region of RANTES is the determinant for activation of the receptor, and portions of the N-loop (among other regions) (from residue 12–22) are important for receptor binding.[12] For

Abbreviations: AIDS, acquired immune deficiency syndrome; AOP, aminooxypentane; AUC, analytical ultracentrifugation; BSA, bovine serum albumin; CCR, CC chemokine receptor; CXCR, CXC chemokine receptor; CHO, Chinese hamster ovary; CNS, crystallography and NMR system; CRPG, chlorphenol red-β-D-galactopyranoside; NNY, *N*-nonanoyl; PSC, [L-ThiaPro2, L-alpha-cyclohexyl-Gly3]; Da, dalton; DSS, 2,2-dimethyl-2-silapentane-5-sulfonic acid; FACS, fluorescence activated cell sorting; FCS, fetal calf serum; FITC, fluorescein isothiocyanate; FBC, fetal bovine serum; HPLC, high performance chromatography; DMEM, Dulbecco's modified Eagle's medium; env, HIV-1 envelope protein; GAG, glycosaminoglycan; HIV, human immunodeficiency virus; HSQC, heteronuclear single-quantum coherence; IL-8, interleukin-8 (also referred to as CXC chemokine Ligand 8 or CXCL8); IPTG, isopropyl-beta-D-thiogalactopyranoside; Kd, dissociation constant; MCP, monocyte chemotactic protein, MCP-1(CCL2), MCP-2 (CCL8), MCP-3 (CCL7) are mentioned in this article; MIP, macrophage inflammatory protein (MIP-1β, CCL4; MIP-1α, CCL3); MW, molecular weight; NMR, nuclear magnetic resonance; PBS, phosphate buffered saline; PBMC, peripheral blood mononuclear cells; PCR, polymerase chain reaction; PEG, polyethylene glycol; PF-4, platelet factor 4 (CXCL4); PI, propidium iodide; RANTES, regulated on activation of normal T cell expressed and secreted (CCL5); RMSD, root mean square deviation; RPMI, Roswell Park Memorial Institute (originally developed the medium RPMI-1640); SDS-PAGE, sodium dodecyl sulfate polyacrylamide gel electrophoresis; SDF-1α, stromal cell-derived factor-1α (CXCL12); TFA, trifluroacetic acid; WT, wild type.

Grant sponsor: NIH; Grant number: R21 AI079777; Grant sponsor: Robert Welch Foundation; Grant number: A1472
*Correspondence to: Patricia J. LiWang, University of California, Merced 5200 N. Lake Road Merced, CA 95343. E-mail: pliwang@ucmerced.edu.
Received 25 March 2009; Revised 18 June 2009; Accepted 30 June 2009
Published online 20 July 2009 in Wiley InterScience (www.interscience.wiley.com).
DOI: 10.1002/prot.22542

example, Pro2, Asp6, Thr7 are involved in activating CCR1, Pro2 and Tyr3 for CCR3, and Tyr3 and Asp6 for CCR5.[12] Regarding receptor binding, it has been found that Arg17 is necessary for RANTES binding to CCR1, Phe12 for binding to CCR3, and Pro2, Phe12 and Ile15 for binding to CCR5.[12] Several N-terminally truncated derivatives, N-terminally extended mutants and N-terminal modification mutants have also been tested and these exhibit antagonist or partial agonist functions. For example, the N-terminal peptide fragments RANTES(1–14),[13] N-loop fragments,[14] as well as the N-terminal truncation mutants RANTES (3–68),[15] RANTES (4–68),[16] RANTES (8–68),[17] RANTES (9–68)[17,18] and RANTES (10–68)[17] were reported to be antagonists in CCR5 binding and to block HIV fusion. Met-RANTES and Leu-RANTES mutants are extended at the N-terminus by one amino acid and show the ability to tightly bind but to not activate CCR5 (or activate very weakly),[19–24] while C1.C5 RANTES also uses only natural amino acids to modify RANTES to obtain strong anti-HIV activity with low agonistic function.[22] Subsequently, a range of N-terminal chemically modified derivatives of RANTES, including AOP-RANTES,[25] NNY-RANTES,[26] and PSC-RANTES,[16,27–29] were widely reported to be highly effective in blocking HIV-1 infection.

In an attempt to improve the ability of RANTES to block HIV entry, a phage display library using randomization of the N-terminal region of RANTES was applied to select RANTES mutants against living cells expressing CCR5.[30] In this work, a potent anti-HIV mutant named P2-RANTES was obtained, having a modified N-terminal sequence: FSPLSSQSS-RANTES (10–68).[30] The chemically synthesized polypeptide of P2-RANTES was shown by these authors to selectively activate CCR5, but not CCR1 or CCR3, in calcium release experiments. A competition assay also revealed that this mutant has improved binding affinity to CCR5 compared to the wild type protein. In an env-mediated cell–cell fusion assay and PBMC infection assay, P2-RANTES resembles AOP-RANTES in function because of its tight binding affinity and strong ability to down-modulate CCR5.[30] However, the structure of P2-RANTES and the manner in which this chemokine variant interacts with CCR5 is unknown. Indeed, until very recently when variations of P2-RANTES were produced,[31] P2-RANTES was the most potent anti-HIV chemokine variant yet discovered that contains all natural amino acids, and is on par with synthetically modified AOP-RANTES and NNY-RANTES. To investigate the structural basis of this unique protein we produced P2-RANTES using *E. coli* overexpression and refolding techniques and solved the structure by x-ray crystallography. The crystal structure of P2-RANTES shows that the N-terminally extended residue, Phe0, plays an important role in the oligomerization and packing. The first 9 residues on the N-terminus of P2-RANTES are clearly defined due to the oligomerization restraints. In particular, the first three residues are well-defined while these residues are generally not defined in NMR and x-ray structures of RANTES.[32–34] Furthermore, we used a cell mediated competition fusion assay to study this protein and found that this recombinant protein is a much more potent HIV fusion inhibitor than C37, a peptide similar to the clinically available fusion inhibitor T-20.[35,36] These findings may aid in the design of potent anti-HIV entry inhibitors and may also be therapeutically useful in the design of antagonists for CCR1 and CCR3.

EXPERIMENTAL PROCEDURES

Chemicals and reagents

All cell culture media, supplements and serum were purchased from Invitrogen (Carlsbad, CA). Fusion inhibitor (*N*-acetylated, C-term amide derivative) C37 was obtained from Genescript. This peptide contains the sequence HTTWMEWDREINNYTSLIHSLIEESQNQQE KNEQELL, which are amino acid residues 225–661 of gp41. Mouse monoclonal antibody to human CCR5 [mouse anti human CCR5 monoclonal antibody from R&D Systems (catalog number: FABSP1, clone: 45,502)] was obtained through the NIH AIDS Research and Reference Reagent Program, Division of AIDS, NIAID, NIH. FITC (fluorescein isothiocyanate) labeled F(ab′)2 fragment of polyclonal goat anti-mouse IgG secondary antibody was purchased from Sigma (catalog number: F 2653).

Cell culture and cell lines

A HeLa cell line stably expressing HIV-1 ADA (R5) env (referred to as HeLa-ADA) was a kind gift from Dr. M. Alizon and Dr. Anne Brelot (Cochin Institute, Paris, France).[37] Cells were cultured in DMEM supplemented with 10% FBS, and 100 units of penicillin and 0.1 mg/mL of streptomycin and the ADA (R5) env was selectively expressed by adding 2 μ*M* methotrexate (Sigma) as previously described.[38] A HeLa cell line stably expressing human receptor CD4 and CCR5 (referred to as HeLa-P5L) was a kind gift from Dr. M. Alizon (Cochin Institute, Paris, France).[37] Cells were cultured in RPMI-1640 (Invitrogen) supplemented with 10% FBS, and 100 units of penicillin and 0.1 mg/mL streptomycin. The expression of CCR5 was selectively expressed by adding zeocin (Invitrogen) at 0.5 mg/mL. The HeLa-TZM cell line was obtained through the NIH AIDS Research and Reference Reagent Program, Division of AIDS, NIAID, NIH: TZM-bl from Dr. John C. Kappes, Dr. Xiaoyun Wu and Tranzyme.[39] These cells were cultured with DMEM supplemented with 10% FBS, 100 units of penicillin and 0.1 mg/mL of streptomycin. The 3T3 cell were cultured in DMEM supplanted with 10% FBS and

with 100 units of penicillin and 0.1 mg/mL streptomycin. The Hela HL2/3 cell line (containing genes from the X4 strain HXB2) was obtained through the NIH AIDS Research and Reference Reagent Program (product number 1294, from Dr. Barbara K. Felber and Dr. George N. Pavlakis) and was cultured in DMEM supplemented with 10% FBS and 500 ug/uL G418.

Protein expression and purification

Wild type RANTES was purified as described previously.[40] For the RANTES mutant P2-RANTES, its corresponding gene[30] with the codons for the addition of a Factor Xa cutting site upstream was amplified through PCR using the wild type RANTES as a template. The PCR product of P2-RANTES was inserted into pET32-Xa (Novagen) at the Nco I-BamH I sites, and the DNA sequence of this mutant was confirmed through DNA sequencing. Protein production was induced by addition of IPTG to 1 m*M* in 37°C culture of BL21(DE3) (Novagen) bearing the constructed plasmid, and the cells were harvested after 7 h by centrifugation at 6000 *g* in an F10S-6X500y rotor (Piramoon Technologies) for 30 min. The cells were resuspended in 30 mL of 500 m*M* NaCl, 20 m*M* Tris (pH 8), and 10 m*M* benzamidine and French pressed twice at 16,000 psi. After centrifugation for 30 min at 17,000 *g* in an SS34 rotor (Sorvall Instruments), the pellet was resuspended in 20 mL of 5 *M* guanidinium chloride, 50 m*M* Tris (pH 8), 500 m*M* NaCl. The solution was stirred overnight and then centrifuged for 30 min at 17,000 *g* to remove remaining insoluble pellet. The soluble denatured proteins were loaded onto a 5 mL Ni chelating column (Amersham Pharmacia Biotech) that was equilibrated with the same buffer [5 *M* guanidinium chloride, 50 m*M* Tris (pH 8), 500 m*M* NaCl]. The denatured proteins were purified through the chelating column using a gradient from 10 to 100% of 500 m*M* imidazole in 5 *M* guanidinium chloride, 50 m*M* Tris (pH 8), 500 m*M* NaCl. The fractions containing purified denatured protein were pooled together and shaken for 2 h at room temperature after adding 10 m*M* β-mercaptoethanol. The purified denatured proteins were dialyzed against 20 m*M* Tris-HCl, pH 8.0 buffer overnight at 4°C to remove denaturant and refold. After dialysis, precipitated matter was removed by centrifugation for 30 min at 15,000 *g* in an F14S-6X250y rotor (Piramoon Technologies) and the protein was purified on a C4 reversed phase chromatography column (Vydac, Hesperia, CA), and lyophilized on a Labconco freeze dry system. To remove the fusion tag, the protein powder was solubilized into ~1 mL of 20 m*M* sodium phosphate (pH 2.5) and the volume was increased to ~40 mL in sterile 20 m*M* Tris (pH 8), 50 m*M* NaCl, and 2 m*M* $CaCl_2$. Factor Xa (Novagen) was used for the proteolytic cleavage, which typically took 2 weeks at room temperature. SDS-PAGE was used to monitor the cutting reaction. Finally, the cut proteins were purified over a C4 reversed phase chromatography column and lyophilized into powder. Protein concentration was quantified by measuring the absorbance at 280 nm using the extinction coefficient method published by Pace.[41] As a control for this method of determining concentration, lyophilized powder was weighed on an Ohaus Voyager balance (Pine Brook NJ), and then dissolved in 10% acetonitrile, 0.01% TFA and its absorbance measured. It was determined that the Pace method overestimated the actual concentration of the protein by about 15% when absorbance was measured on a Beckman DU 640 spectrophotometer (Fullerton, CA), and by about 30% when absorbance was measured on a Nanodrop spectrophotometer (Nanodrop/ThermoScientific Wilmington, DE). However, there was some variability in the actual measurement of the weight of protein powder given the small amounts involved, so the well-established Pace method was used in the results reported here.

Crystallization of P2-RANTES

The lyophilized P2-RANTES sample was resuspended in 0.05% TFA at a concentration of 2 mM. 2 μL of this protein solution was mixed with 2 μL of precipitant: 50 m*M* Bis-Tris, pH 5.5, 200 m*M* ammonium sulfate, 20% PEG3350. Crystals were grown in hanging drops using a 48 well crystal screen plate (Hampton) with the reservoir solution being the same as the precipitant. Small monoclinic crystals were grown in 1–2 days and allowed to continue to grow for about 1 week to get ready for diffraction data collection. The crystal was soaked stepwise in a mother-liquor containing 5–25% glycerol and flash frozen in liquid nitrogen. The diffraction data was collected using an RAXIS IV image plate detector mounted on a Rigaku Micromax-007HF generator. The P2-RANTES crystal belongs to C2 space group with four molecules in the crystallographic asymmetric unit. The diffraction data was processed with the HKL2000 suite. Statistics of the diffraction data are listed in Table I.

Structural determination and refinement

The structure of P2-RANTES was determined by molecular replacement using the structural model of AOP-RANTES (PDB id: 1B3A) as a search model. The first 10 residues were deleted from the search model. Four molecules of the search model were located in the unit cell using the program MOLREP in the CCP4 suite.[42] The solution was improved by rigid body refinement using CNS.[43] The electron density map calculated from the model after rigid body refinement showed clear and complete electron density for the first 10 residues for one of the mutant molecules and fragmented density for another molecule. No electron density was observed for the first nine residues of the other two molecules in the asymmetric unit, which are presumed to be disor-

Table I
Data Collection and Refinement Statistics. Data were Collected from a Single Crystal for Each Structure

	P2-RANTES
Data collection	
Space group	C2
Cell dimensions	
a, b, c (Å)	116.68, 51.98, 61.69
α, β, γ (°)	90, 117.87, 90.0
Resolution (Å)	50–1.70 (1.76–1.70)
R_{merge}	4.6 (19.9)
I/σI	49.9 (6.5)
Completeness (%)	97.4 (79.6)
Redundancy	3.4 (2.5)
Refinement	
Resolution (Å)	50–1.70
No. reflections	34,463
R_{work}/R_{free}	21.7/24.8
No. of atoms	
Protein	2123
Ligand/ion	
Water	313
B-*factors*	
Protein	36.0
Ligand/ion	
Water	50.4
R.m.s. deviations	
Bond lengths (Å)	0.010
Bond angles (°)	1.56

Values in parentheses are for highest-resolution shell.

dered. The molecular model was completely rebuilt for the first 10 residues of molecule A and B according to $2|F_o|-|F_c|$ simulated annealing omit map. The model was refined by several cycles of positional refinement and remodeling. In the final stage of the refinement, individual B factors were refined and solvent molecules were added to peaks higher than 3σ in the difference map. The crystallographic *R* factor for the final model is 21.7% and R_{free} is 24.8%, with good geometry. Statistics of the crystallographic data and refinement are listed in Table I.

Analytical ultracentrifugation

Sedimentation equilibrium and sedimentation velocity measurements were carried out with a temperature-controlled Beckman XL-I analytical ultracentrifuge equipped with an An-60 Ti rotor and a photoelectric scanner (Beckman Instruments, Palo Alto, CA). For equilibrium experiments, varying concentration (20, 25, and 35 μ*M*) of P2-RANTES were dissolved in buffer containing 50 m*M* Bis-Tris, pH 5.5, with 200 m*M* NaCl. In some cases ^{15}N P2-RANTES was used, since this material is also suitable for NMR. However, the overall conclusions regarding oligomeric state were identical to the use of ^{14}N P2-RANTES. Samples were loaded onto a 12 mm aluminum six channel centerpiece and run at 35,000, 45,000, and 55,000 rpm at 20°C for 16 h for each speed in a step scan model. For velocity experiments, 40 μ*M* of P2-RANTES was dissolved in buffer containing 50 m*M* Bis-Tris, pH 5.5, with 1000 m*M* NaCl. The protein sample was loaded in a double sector 12 mm aluminum centerpiece and at a rotor speed of 60,000 rpm at 20°C for 24 h in a continuous scan model. For both equilibrium and velocity experiments, the reference compartments were loaded with the matching buffer without proteins and samples were monitored by absorbance at 280 nm. Analysis of the raw data was carried out using UltraScan version 8.0 (http://www.ultrascan.uthsca.edu). The partial specific volume of P2-RANTES was estimated using the amino acid composition methods implemented in UltraScan. The Hydrodynamic corrections for buffer conditions were calculated by UltraScan. For the equilibrium experiments, data were analyzed using the Global Nonlinear Least-Squares fitting methods implemented in UltraScan. The equilibrium data were also analyzed using the program Origin (Beckman), and the results were found to be very consistent with those from UltraScan. For velocity experiments, data were analyzed using the enhanced van Holde-Weschet method in UltraScan.[44,45]

Nuclear magnetic resonance

^{15}N labeled wild type RANTES and P2-RANTES were produced in minimal medium with $^{15}NH_4Cl$ as the sole nitrogen source. The purified lyophilized powders were dissolved in 10% D_2O with 20 m*M* sodium phosphate, pH 2.8 (wild type RANTES) and pH 3.0 (P2-RANTES). The samples were placed in Shigemi tubes (Allison Park, PA) and the spectra referenced relative to DSS (2,2-dimethyl-2-silapentane-5-sulfonate).[46] NMR spectra were acquired at 25°C on a Varian Unity Plus 500 MHz spectrometer equipped with an *xyz* gradient penta probe. ^{15}N-^{1}H HSQC (heteronuclear single quantum coherence) spectra were collected with 512* points in the proton dimension and 128* points in the nitrogen dimension. The data were processed using the program nmrPipe[47] and analyzed using the program PIPP.[48] The selected assigned peaks are labeled using the information from the previously published NMR data.[33]

Cell–cell fusion assay

Envelope-mediated cell–cell fusion assays were carried out as described in reference[37,38] with HeLa-P5L and HeLa-ADA cell lines with minor modification. Briefly, 10^4 HeLa-P5L cells were seeded in 96-well culture plate in 50 μL RPMI-1640 medium per well for 4–5 h. For the 3T3 competition assay, an equal number of HeLa-P5L and 3T3 cells were mixed such that the total concentration of cells were 10^4 per well (0.5×10^4 each) in 100 μL RPMI-1640 medium. After 12–14 h of incubation the medium was aspirated and replaced with 50 μL RPMI-1640 medium. The sample of P2-RANTES or C37 was added into the cell medium with serial dilution from 428 n*M* to 66 pM (protein concentration was quantified

by measuring the absorbance at 280 nm from a concentrated stock). After preincubation at room temperature for 10 min, 50 μL HeLa-ADA (10^4 cells per well) in RPMI-1640 medium were added into the 96-well culture plate. After a further 24 h of incubation at 37°C for complete fusion, the medium was aspirated and the cells in the 96-well culture plate were lysed by adding 20 μL 0.5% NP-40 (US Biological) in PBS for 30 min at room temperature and assayed for β-galactosidase activity by the addition 30 μL of 8 m*M* substrate CRPG (Sigma) in PBS with 20 m*M* KCl and 10 m*M* β-mercaptoethanol for 1–2 h in the dark at room temperature. The absorbance at 570 nm (using a reference wavelength of 630 nm) was read on a microplate reader (Biotek). The percentage of the cell–cell fusion was expressed as 100x (mean absorbance of treated well—mean absorbance of HeLa-P5L only well)/(mean absorbance of untreated well—mean absorbance of HeLa-P5L only well). Experiments were performed in triplicate, in three or more independent experiments, and dose dependent inhibition curves were fitted with a four-parameter logistic equation[49] using KaleidaGraph (version 3.6, Synergy Software).

Pseudotyped viral assay

293 FT cells were cotransfected with pNL luc3 R- E- and pSV-ADA or pSV-JRFL[50] (a kind gift from Dr. Nathaniel Landau) according to the transfection reagent manual (ProFection® Mammalian Transfection System – Promega). Supernatants containing virus were collected 48 h post-transfection, spun down and filtered with 0.45 μm syringe filters to remove viral clusters. The virus produced in this system is infectious for one round only, because the genes for the viral surface proteins (env genes) are on a vector (not the genome) and are therefore not transmitted to progeny virus after infecting a target cell. For viral titration, Quick Titer Lentivirus Quantification Kits were used. 10^4 TZM cells/well were infected with 50–100 ng p24/well. After 48 h of incubation, cells were lysed and assayed using the Promega Luciferase assay system. 96 well plates were read using an Orion II microplate luminometer (Berthold Techniques, Germany).

FACS analysis

HeLa-TZM cells (10^5) were incubated for 30 min at 37°C in culture medium containing various concentration of (0–100 n*M*) of reagents (i.e. P2-RANTES) in 10 × 75 mm culture tubes (Fisher Scientific). After washing 4 times with 10 mL cold PBS, cells were incubated in 300 μL of 500 μg/mL mouse anti-human CCR5 monoclonal antibody in PBS-0.5% BSA (Sigma), and kept on ice for 45 min. The cells were then washed three times with cold PBS-0.5% BSA and incubated in 300 μL of 50 μg/mL FITC labeled polyclonal goat anti-mouse antibody in PBS-0.5% BSA, and kept on ice for 30 min. One aliquot of untreated cells were incubated with PBS-BSA for 30 min followed by three washes and incubation with the FITC-labeled goat anti-mouse IgG as a control. Then the cells were washed three times with cold PBS-0.5% BSA and kept in PBS-0.5% BSA, and analyzed with a FACSCalibur (BD Biosciences, SanJose, CA) flow cytometer using CellQuest (BD Biosciences) acquisition software. Cell viability was determined by staining with propidiumiodide (PI) at 1 μg/mL final concentration 1 min before analysis. FITC fluorescence was collected through a 515/30 band pass filter, and PI fluorescence through a 650LP filter. List mode data were acquired on a minimum of 10,000 viable cells defined by a light scatter and lack of PI staining. Data were analyzed using FlowJo (Tree Star, Ashland, OR). First, a region to define cells was set using a forward and side light scatter plot, then viable (PI-negative) cells were determined by a plot of forward light scatter and PI fluorescence. Results are presented as histograms of FITC fluorescence.

Heparin sepharose chromatography

GAG binding capacity of chemokine mutants was studied by using heparin Sepharose chromatography as mentioned in previous publications.[51] Briefly, wild type RANTES or P2-RANTES (~10 μg of lyophilized protein) was taken up in 0.5 mL of 50 m*M* Tris (pH 7.4) and injected onto a 1 mL Hi-Trap heparin column (Pharmacia) using the AKTA HPLC system (GE Healthcare). The column was equilibrated with 5 mL of the same buffer followed by a gradient of 0 to 1200 m*M* NaCl in 50 m*M* Tris (pH 7.4) at a rate of 0.5 mL/min for 60 min. The elution profile was monitored by UV absorbance at 280 nm. The salt concentration corresponding to the center of each eluted peak is an indication of the GAG binding ability of that protein. Each experiment was repeated two times.

RESULTS

Protein production and characterization

P2-RANTES was largely an inclusion body when overexpressed in the *E. coli* strain BL21 (DE3). After refolding, the soluble His-tagged protein was purified using a Ni affinity column followed by reversed phase chromatography. After removal of the N-terminal tag using Factor Xa to maintain the exact N-terminal of P2-RANTES sequence, the soluble tag-free protein was finally purified using reversed phase chromatography. The mass spectrum of P2-RANTES indicated that the protein was nearly 97% pure, with a molecular weight of 7894 ± 8 Daltons (data not shown). This compares well with the molecular weight of 7906 Dalton calculated from the amino acid composition of native P2-RANTES, and

indicates that P2-RANTES produced by *E. coli* overexpression has the correct sequence, including the critical N-terminal region. The tag-free P2-RANTES was also determined to be folded, as judged by ^{15}N HSQC experiments (measured on ^{15}N isotopically labeled protein), which show good dispersion in the ^{1}H dimension [Fig. 1(A)]. The overlay of the spectrum of P2-RANTES with wild type RANTES shows many peaks in similar positions, indicating structural similarity between the two proteins, although, as will be discussed, the two proteins likely differ in quaternary state in solution.

Anti-HIV function

To test the biological function of P2-RANTES produced from the *E. coli* overexpression, we carried out a cell–cell fusion assay that is an accepted model of R5-tropic HIV infection.[38] In the fusion assay, the IC_{50} for P2-RANTES is 2.4 ± 0.8 n*M* [Fig. 1(B)]; the figure shows data in the presence and absence of competition (described below). This is similar to the published results using P2-RANTES produced by complete chemical synthesis (0.6, 1.6 n*M*).[30,31] In our assay, the fusion inhibitor peptide C37 showed an IC_{50} of 18.2 ± 7.5 n*M*. This result indicates that the bacterially produced P2-RANTES is fully functional and is a significantly better inhibitor than the commonly used C-peptide. As expected, P2-RANTES was unable to inhibit cell fusion in a system using gp120 from HXB2, an X4 tropic HIV strain (data not shown).

The recombinantly produced P2-RANTES was also tested in single round infection assays using virus pseudotyped with the R5 strains ADA and JRFL. In both cases, P2-RANTES performed well, exhibiting an IC_{50} for inhibition of infection of 0.58 ± 0.22 n*M* for the ADA strain, and 0.46 ± 0.035 n*M* for the JRFL strain [Fig. 1(C)]. These assays are sensitive to the cell type that is infected, and preliminarily, P2-RANTES exhibits even better inhibitory capability when used with other cell types (data not shown).

In addition to the conventional cell–cell fusion assay, we modified the experiment to include the presence of unrelated cells (referred to as competition with "unrelated" cells) to detect whether P2-RANTES exhibits specificity. Several studies indicate that in addition to its HIV gp41 target, the clinically used T-20, a C-peptide which shares a large portion of sequence with C37, can also bind to undefined targets such as cell membrane or lipids.[52–55] This possible lack of specificity could be one reason that T-20 requires a very high dosage for clinical use. In this competition assay, in addition to the cells involved in fusion, we added mouse 3T3 cells, which do not contain human CD4, CCR5 or HIV env on the surface. These cells could act as a competitor for nonspecific binding, but should have little or no effect on a fusion inhibitor with specificity for the fusion complex. With the 3T3 cells present (0.5×10^4 3T3 cell/well, 1×10^4 HeLa-ADA/well, 0.5×10^4 HeLa-P5L/well), C37 was shown to have a significantly reduced inhibitory capacity, with an IC_{50} of 61.4 ± 7.9 n*M* [Fig. 1(B)]. As a control, 3T3 cells were shown not to affect the fusion process or the speed of fusion (data not shown). Overall, the approximately three-fold decrease of potency in the inhibition of cell–cell fusion by C37 is apparently due to the presence of 3T3 cells. Interestingly, in the same type of experiment, P2-RANTES was shown to have an IC_{50} of 0.94 ± 0.5 n*M* when 3T3 cells are present [Fig. 1(B)], which is unchanged from an IC_{50} of 0.91 ± 0.5 n*M* which is obtained when the assay is done with the same number of cells but lacking the 3T3 competitor cells. (The assay is sensitive to the number of cells used, which is why these numbers are slightly different than those reported above.) This indicates that in a complex environment, P2-RANTES may be targeted to the proper cells better than other fusion inhibitors, allowing overall lower doses for clinical effectiveness.

CCR5 down modulation

As mentioned by Hartley et al.[30] there are two mechanisms underlying the improved anti-HIV activity of P2-RANTES compared to wild type RANTES: increased binding affinity for CCR5 (allowing it to block access to CCR5), and enhanced capacity in removing CCR5 from the surface of the cell, rendering CCR5 unavailable for interaction with the HIV surface proteins. To provide evidence for the ability of P2-RANTES to down-modulate CCR5, we carried out CCR5 internalization experiments monitored by FACS, similar to those of Hartley et al. but with a different cell line. As shown in Figure 1(D), P2-RANTES strongly internalized CCR5 on HeLa-TZM cells in a concentration dependent manner, while the wild type RANTES control did not show significant changes in CCR5 surface expression in the same experiment. The reason for low internalization by wild type RANTES is likely due to the fact that these experiments were carried out on nonleukocytic cells, and incubation times were short. Indeed, these results are in agreement with the previously published work with different CCR5 expression cell lines using the synthesized P2-RANTES polypeptide and wild type RANTES.[30]

GAG binding studies

Most chemokines are highly positively charged. This property facilitates the binding to GAGs on the surface of cells, which immobilize and present the chemokine, possibly aiding in the establishment of chemokine concentration gradients for leukocyte chemotaxis.[1,56–58] The role of GAG binding by chemokines in their anti-HIV activity is not clear. Although the amino acids in RANTES that most directly affect GAG binding are in

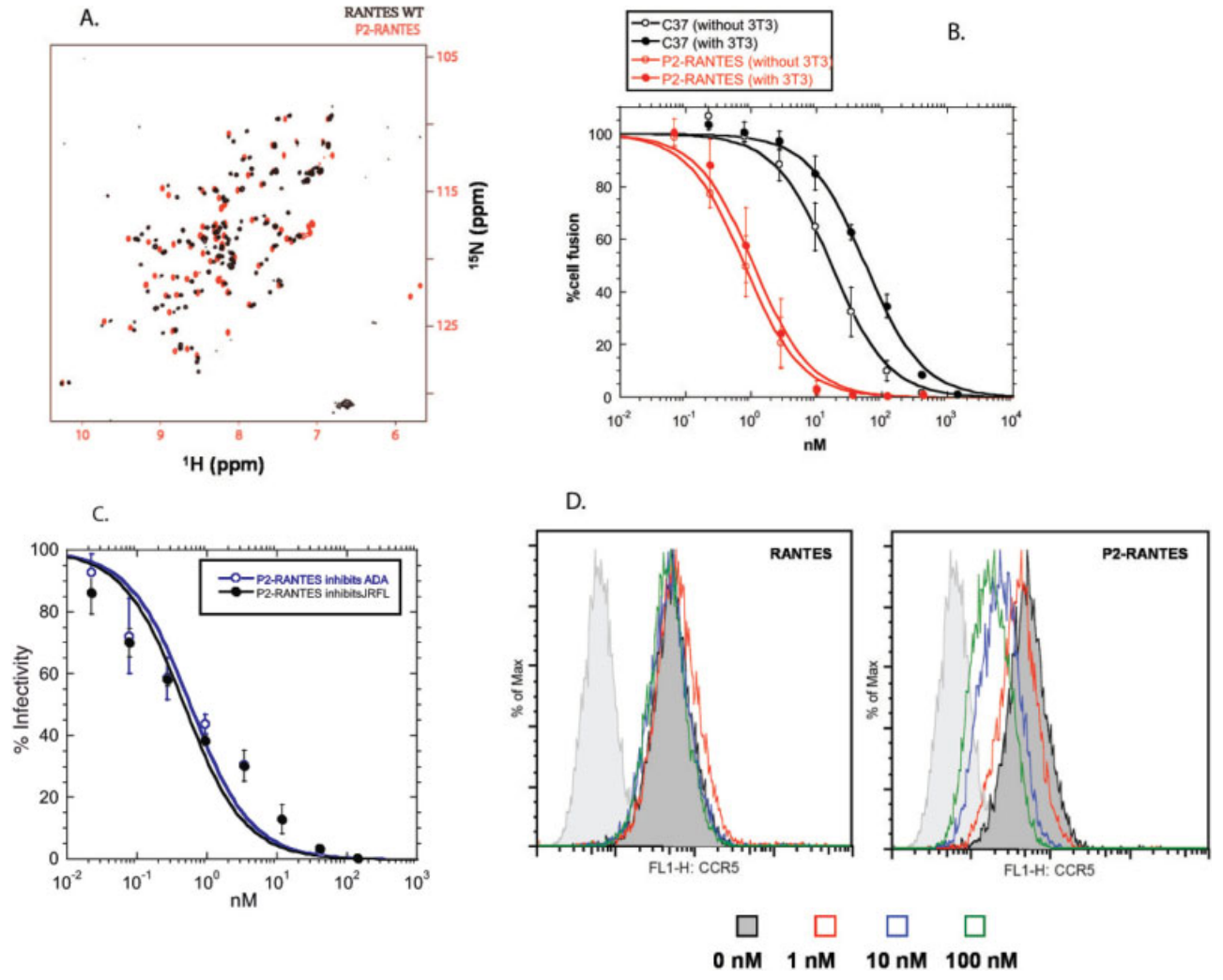

Figure 1

Characterization and functional studies of P2-RANTES (**A**) The ^{15}N HSQC spectrum of wild type RANTES (black) and P2-RANTES (red). (**B**) The inhibition of HIV-1 fusion plotted as the percentage of fusion versus the concentration (n*M*) of inhibitor in the HeLa-ADA and HeLa-P5L R5 tropic cell–cell fusion assay: C37 (without 3T3 cell competition, black open circles; with 3T3, black filled circles); P2-RANTES (without 3T3 cells, red open circles; with 3T3 cells, red filled circles). Experiments were done in triplicate and repeated at least two times. Data shown is the average of all the experiments. Error bars indicate the standard deviation (±SD). Curves were fitted using KaleidaGraph. Without 3T3 cells, the 50% of fusion inhibition (IC_{50}) for C37 and P2-RANTES are 17 ± 4.7 n*M* and 0.91 ± 0.5 n*M* respectively; With 3T3 cells, the IC_{50} for C37 and P2-RANTES are 61.4 ± 7.9 n*M* and 0.94 ± 0.5 n*M* respectively. The experiment is sensitive to number of cells used such that when 10^4 target cells were used, P2-RANTES inhibited with an IC_{50} of 2.4 ± 0.8 n*M*, which is also described in "Results" section. (**C**) The inhibition by P2-RANTES of single round virus pseudotyped with either the ADA strain (blue) or the JRFL strain (black). Data shown are the average of two independent experiments done in triplicate. Error bars indicate standard deviation. (**D**) CCR5 internalization induced by wild type RANTES and P2-RANTES in a steady–state CCR5 down modulation FACS experiment. Data were plotted as histogramsof fluorescence intensity (cell surface CCR5), with the cell number normalized for each sample. FITC fluorescence intensity from different concentrations of drug treated HeLa-TZM cells (stained with the same CCR5 antibody and secondary antibody) are presented in different colors: black (0 n*M*); red (1 n*M*); blue (10 n*M*) and green (100 n*M*). The cells stained without CCR5 antibodies are showed as a gray curve.

the 40's loop of the protein and not particularly important in CCR5 binding,[59] the N-terminus of RANTES (which is critically important in CCR5 function and anti-HIV activity) appears to also play a role in GAG binding.[59,60] In addition, the dimerization of CC chemokines is mediated by their N-terminal amino acids, and it has been shown that the ability to dimerize is directly related to GAG binding ability.[40,61] Therefore, changes in the N-terminus of CC chemokines, such as those that lead to P2-RANTES, have the potential to affect the GAG binding ability of the protein as well as its oligomerization state and ability to inhibit HIV. Previous studies have suggested that AOP-RANTES may have different GAG binding capability than Met-RANTES.[34] To determine whether P2-RANTES (which is extensively mutated at the N-terminus compared to

RANTES) has altered GAG binding capacity, heparin chromatography was carried out at pH 7.4. As shown in Figure 2(A), elution of wild type RANTES from the heparin column was found to require 700 m*M* NaCl, while P2-RANTES requires only about 550 m*M* NaCl. This suggests that P2-RANTES indeed has a lower capacity to bind glycosaminoglycans compared to the wild type RANTES.

Analytical ultracentrifugation sedimentation

Similar to other chemokines, RANTES can dimerize in solution,[32,33] and this property has been shown to be critical for *in vivo* function and is likely to play an important role in regulation of GAG binding.[40,62,63] Because P2-RANTES has many N-terminal amino acid residues mutated from the wild type protein, and the N-terminal region of the protein is critical for dimerization, this may indicate that P2-RANTES has a different oligomerization state than wild type RANTES. We carried out analytical ultracentrifugation sedimentation equilibrium and velocity experiments to determine the quaternary structure of P2-RANTES. Our results with multiple concentrations and multiple speeds suggest that P2-RANTES is predominantly monomeric in solution. As shown in Figure 2(B), the sedimentation equilibrium experiments revealed that P2-RANTES fits best to a single component model. The data do not fit to either a monomer-dimer equilibrium or monomer-tetramer equilibrium model. The fitted molecular weight is around 7.7 kDa in 200 m*M* NaCl, buffered with 50 m*M* Bis-Tris at pH 5.5. Since ours and other studies suggested that chemokine oligomerization is salt dependent,[40,61,64-66] we carried out further sedimentation velocity experiments with higher salt: 1000 m*M* NaCl in 50 m*M* Bis-Tris, pH 5.5. Using the program UltraScan,[44,45] the sedimentation data was transformed into a species population plot. As shown in Figure 2(C), 90% of the population of P2-RANTES under these conditions is a monomer, and 10% of the population is dimer. This again indicates that P2-RANTES is predominantly a monomer that has a weak tendency to dimerize in certain conditions (such as in a high concentration of salt).

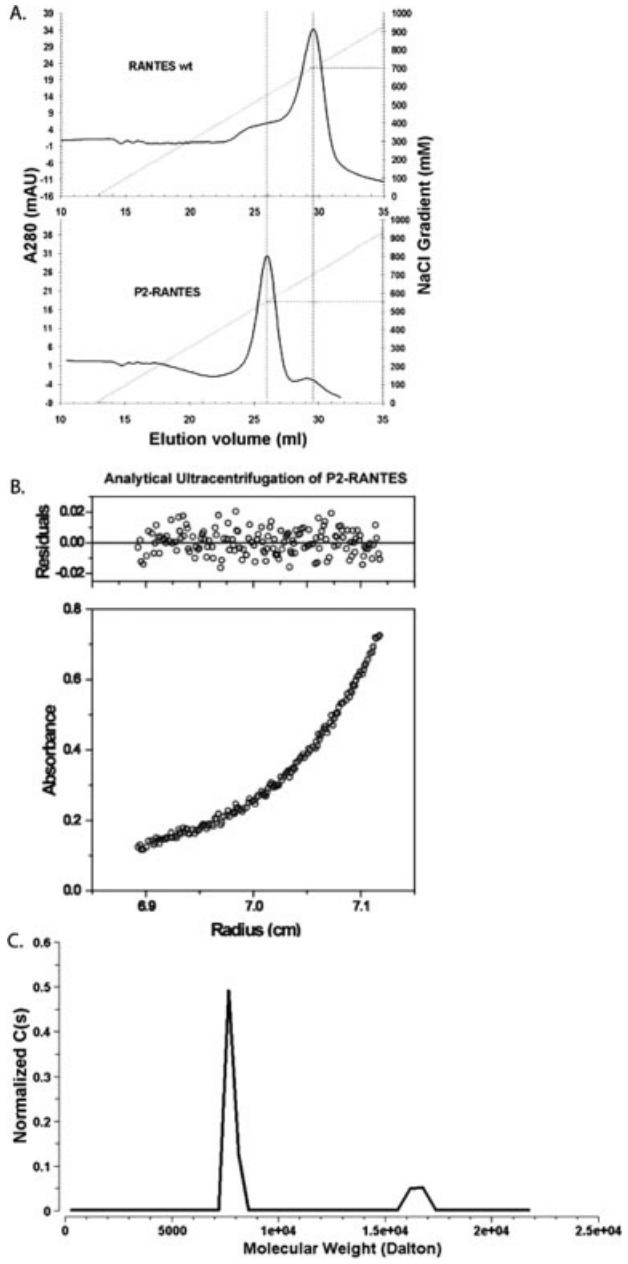

Structure determination and description

The overall crystal structure of P2-RANTES is well-defined at 1.7 Å resolution with an *R* free factor of 24.8% (Table I). The overall structure of P2-RANTES is a homotetramer containing four subunits labeled A, B,

Figure 2

GAG binding and oligomerization state of P2-RANTES in solution. (**A**) Heparin sepharose chromatography of wild type RANTES and P2-RANTES. Equal amounts of wild type RANTES and P2-RANTES were loaded onto a heparin sepharose column and eluted using an NaCl gradient. The dash lines indicate the NaCl concentration required for elution: 700 m*M* for wild type RANTES and 550 m*M* for P2-RANTES. (**B**) Analytical Ultracentrifugation sedimentation equilibrium experiment of P2-RANTES (24 μ*M* protein in 50 m*M* Bis-Tris, 200 m*M* NaCl, pH 5.5, at 55,000 rpm) is shown as a plot of absorbance at 280 nm versus radial distance. The data is fit with a single component model with a fitted molecular weight (MW) of 7.7 kDa (Origin 3.78, Beckman). The calculated molecular weight from amino acid composition is 7.9 kDa. (**C**) Analytical ultracentrifugation sedimentation velocity experiments of P2-RANTES were carried out at very high salt concentration to promote dimerization. This representation of the data shows the population of each species versus molecular weight. The molecular weight distribution of P2-RANTES at 50 m*M* Bis-Tris, pH 5.5, 1000 m*M* NaCl indicates that 90% population is in the monomer form (around 8 kDa) and 10% of the population is in the dimer form (around 16 kDa).

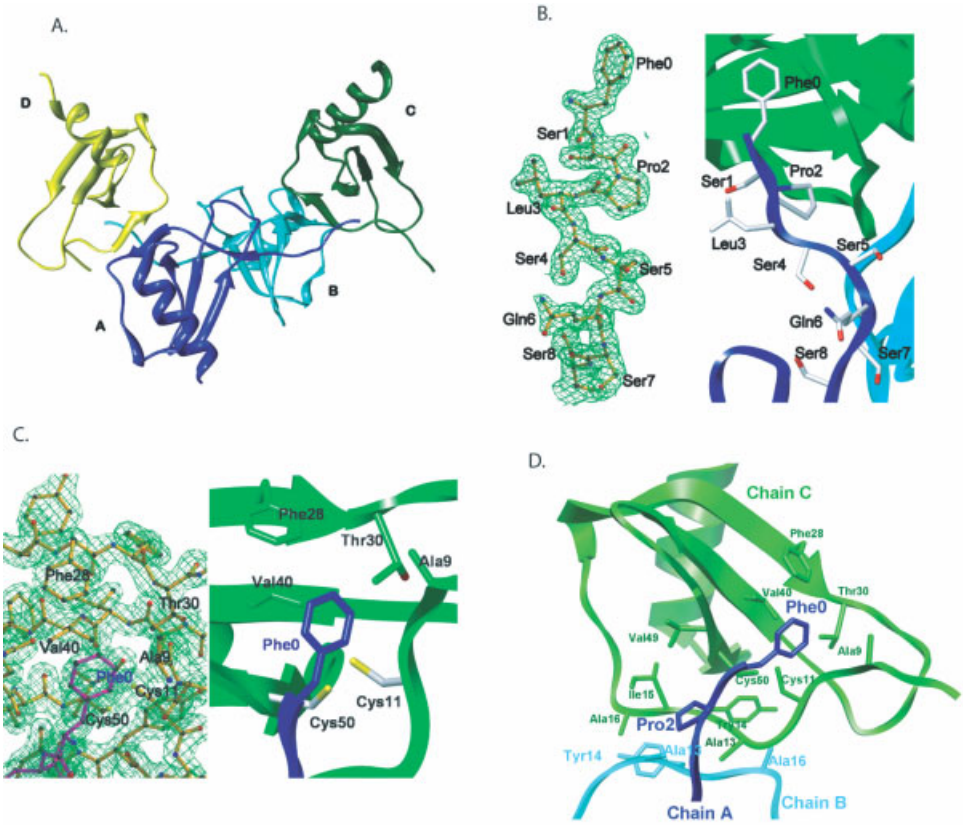

Figure 3

Structure of P2-RANTES. A. Overall structure of the P2-RANTES tetramer in the crystallographic asymmetric unit. The four monomers are colored blue (**A**), cyan (**B**), green (**C**), and yellow (**D**), respectively. B. Close-up view of the N-terminal residues of monomer A. $2|F_o|-|F_c|$ electron density map contoured at 1.0 σ near the N-terminus of monomer A (left) showing the well-defined structure of residues from Phe0 to Ser8 (yellow stick models). On the right side, these N-terminal residues are shown in blue ribbon with white stick models. C. Close-up view of the interface between monomer A and the hydrophobic pocket of monomer C. $2|F_o|-|F_c|$ electron density map contoured at 1.0 σ (left) showing the interactions between the N-terminus residue Phe0 (blue stick models) of monomer A with residues Phe28, Thr30, Ala9, Val40, Cys11, and Cys50 (yellow stick models) of monomer C. On the right side, the blue Phe0 is shown interacting with monomer C (green ribbons and green stick model). D. Close-up view of the interface between monomer B and monomer C. Hydrophobic interactions between residues Tyr14(B) and Ala16(C), Ala16 (B) and Tyr14(C), are observed between monomer B (cyan ribbon) and C (green ribbons). Residue Pro2 (blue stick model) of monomer A (blue ribbon) also contacts Ile15, Val49, and Ala13 (green stick model) of monomer C. All the ribbons figures were generated using Chimera.[67]

C, and D [Fig. 3(A)]. Chain A and chain B have completely defined structures from residues Phe0 to Ser 68. The electron density map of the N-terminal region in chain A and B is clearly defined [Fig. 3(B)]. The N-terminal region in chain C (Phe0-Ser4) and chain D (Phe0-Ser5) is disordered, but the rest of the core structure (chain C: Ser5 to Ser68; chain D: Ser7-Ser68) are well-defined.

All the monomeric subunits of P2-RANTES from chain A to D share the same tertiary structure as other CC and CXC chemokine monomers, with three antiparallel β strands and an α-helix connected to the third β-strand via a flexible loop. Two left-handed disulfide bridges (Cys10-Cys34, Cys11-Cys50) restrain the overall conformation of the core of the chemokine fold. A short β-sheet (β0) is formed in the monomers of chain A and chain B from residues Ser8 to Cys10. This region mediates the dimerization in wild type of RANTES,[32–34,68] but wild type RANTES has Pro9 in the middle of the small dimerization β sheet, while P2-RANTES has Ala9 in the middle instead. This may make the β0-β0 dimer in P2-RANTES slightly weaker than wild type RANTES. All four monomers contain a long loop (N-loop, or sometimes referred to as the 20's loop) between Cys11 and Pro20. This loop region has been postulated to be a major determinant of binding to CCR5.[12,14,64,69,70] After a short 3^{10} helix (Arg21–His23), there are three main antiparallel β-strands formed by Ile24–Tyr29 (β1), Val39–Thr43 (β2) and Gln48–Ala51 (β3). Then each monomer shows a C-terminal α-helix (α1) formed by

residues from Lys56 to Glu66, followed by extended residues Met67 and Ser68. The loop between β1 and β2 (Ser31–Cys34, or sometimes referred to as the 30's loop) contains a Type III reverse turn; the loop between β2 and β3 (Thr43–Asn46, sometimes referred to as the 40's loop) contains a Type I reverse turn; and the loop between β3 and β1 (Asn52–Lys55, or sometimes referred to as the 50's loop) is a Type I reverse turn.

The central dimer in the structure between subunits A and B is similar to other determined CC chemokine dimer interfaces, including that of wild type RANTES.[32,33] For example, antiparallel β0-β0 interactions are formed by residues Ser8-Ala9-Cys10, hydrogen bonds are formed between Ser7 (N) and Gln48′ (O), Ser7 (OG) and Gln48′ (OE1), Ser8 (N) and Cys10′ (O), Cys10 (N) and Ser8′ (O), Cys50 (N) and Ser 5′ (O). This is slightly different from the AOP-RANTES and Met-RANTES structures in which the hydrogen bonds are formed between Ser5 (O) and Cys50′(N), Asp6(N) and Gln48′(O) and Thr7(OG1) and Gln48′(OE1).[34] Phe12 is well-known to be critical for binding to CCR5 and for dimerization.[14] In the P2-RANTES dimer between chain A and chain B, Phe12 is observed to make the usual dimer interactions as seen in other CC chemokine dimers. Comparison of the N-termini from both monomers shows the N-terminus of monomer A to be better resolved and more highly ordered than monomer B, with clearer density and lower temperature factors (Fig. 3).

The interaction of the peripheral subunits (C and D) with the central dimer (subunits A and B) are not typical of either a CC or CXC intersubunit interaction. These "tetramer interactions" appear to be weaker and mediated by the N-terminus of P2-RANTES. While both monomeric and dimeric forms of CC chemokines have been shown to be physiologically relevant,[62] the tetrameric form may be an artifact of crystallization, particularly since the present work shows that the predominant form in solution is a monomer, with some contribution of dimer. However, an analysis of the tetramer can be briefly described as follows: the N-terminus of P2-RANTES is extended in length compared to the wild type protein, with an N-terminal Phe termed Phe0. This residue Phe0 from chain A (or chain B) makes contact with hydrophobic clefts on chain C (or chain D). As shown in Figure 3(C), based on the electron density map, Phe0 from monomer A makes hydrophobic interactions with Phe28, Thr30, Ala9, Val40, Cys11, Cys50 of monomer C. The residue Pro2 of chain A (or B) is also found to contact to Ile15, Val49 and Ala13 of chain C (or D). Monomer B and C interact with each other predominantly through backbone hydrogen bonds between residues Phe12, Tyr14, and Ala16 in the two molecules. Hydrophobic interactions between residues Tyr14 (chain B) to Ala16 (chain C), Ala16 (chain B) to Tyr14 (chain C) were also observed at the interface between monomer B and C [Fig. 3(D)].

Table II
The Buried Surface Area of Dimer Interface

RANTES variants		Monomer 1 (Å^2)	Monomer 2 (Å^2)	Dimer (Å^2)	Buried surface area (Å^2)
P2-RANTES	A–B	5242	5286	9064	1464
	A–C	5242	4692	9318	616
	A–D	5242	4609	9082	769
	B–C	5286	4692	9131	847
	B–D	5286	4609	9257	638
RANTES wt (1hrj)		5451	5429	9142	1738
AOP-RANTES (1b3a)		5125	4917	8081	1961

Calculations were made using UCSF Chimera.[67]

However, the buried surface area of these A/C or B/D interfaces are much smaller than the dimer interface between monomer A and B (Table II).

Comparison of P2-RANTES structure with other crystal structures of RANTES

There is very little difference in the tertiary structure between the crystal structure of P2-RANTES described here and the crystal structures of Met-RANTES[71] and AOP-RANTES.[68] The root mean square deviation (rmsd) values for superpositioning the backbone atoms of P2-RANTES residues 6–68 onto the equivalent atoms of the 1eqt (Met-RANTES) and 1b3a (AOP-RANTES) structures are 0.461 Å and 0.461 Å, respectively. However, there is a great deal of difference in the N-terminal regions of the monomeric subunit as seen in the overlay of these three crystal structures [Fig. 4(A)]. In contrast to the Met-RANTES structure, in which the conformation of the first three residues was not determined, the extended Phe0, Ser1, Pro2, and Leu3 are seen quite clearly in the P2-RANTES crystal structure between subunit A and subunit B [Fig. 3(B)].

The largest differences among the various RANTES analogs appear to be in the dimer interface. In Figure 4(B), the monomer A from P2-RANTES was used as a reference, and all dimer structures (using subunit A and B in P2-RANTES) were superimposed using UCSF Chimera.[67] The monomer–monomer orientation in the dimer of P2-RANTES (red) is somewhat different than AOP-RANTES (purple) or Met-RANTES (gray). In particular, the changes in the N-terminal region propagate to the C-terminus, resulting in the C-terminal α-helix being oriented away from the referenced monomer. Also, Phe0 of P2-RANTES (red stick model) is pointing in a very different direction compared to the AOP group (purple stick model) in AOP-RANTES. Other residues including Ser1, Pro2, and Tyr3 (in P2-RANTES this is Leu3) also show different orientations. The fewer contacts between the subunits of P2-RANTES seem to allow the dimer to flex, as seen in a comparison of the P2 RANTES dimer with Met-RANTES and AOP-RANTES.

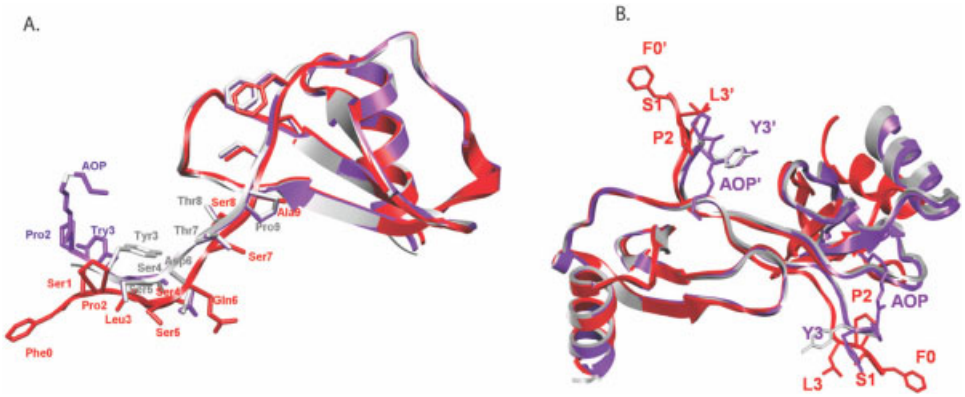

Figure 4

Comparison of P2-RANTES structure to other crystal structures of RANTES. **(A)** Overlay of the monomer structure of P2-RANTES (red) with Met-RANTES (gray, pdb file: 1eqt) and AOP-RANTES (purple, pdb file: 1b3a). The conserved four Cys residues were used to superimpose the monomer structure of these three using the "super match" function in UCSF Chimera.[67] **(B)** Overlay of the dimer structure of P2-RANTES with Met-RANTES and AOP-RANTES. The monomer A from P2-RANTES was used as a reference, and all dimer structures (using subunit A and B in P2-RANTES) were superimposed using UCSF Chimera.[67] The monomer–monomer orientation in the dimer of P2-RANTES (red) is somewhat different than AOP-RANTES (purple) or Met-RANTES (gray). In particular, the changes in the N-terminal region propagate to the C-terminus, resulting in the C-terminal α-helix being oriented away from the referenced monomer. Also, Phe0 of P2-RANTES (red stick model) is pointing in a very different direction compared to the AOP group (purple stick model) in AOP-RANTES. Other residues including Ser1, Pro2, and Tyr3 (in P2-RANTES is Leu3) also show different orientations. All figures were made using UCSF Chimera.[67]

The dimeric structure of P2-RANTES is less compact than the AOP-RANTES structure, as reflected in the total buried surface area [Table II; Fig. 4(B)]. AOP-RANTES buries 24% of the total monomeric solvent accessible surface upon dimerization, and wild type RANTES buries 19% in the determined dimer, whereas P2-RANTES buries only 16% (Table II). The difference in the buried surface area between P2-RANTES and AOP-RANTES, which likely accounts for the weaker dimer in P2-RANTES, is due mainly to the tight fit between the Pro2 and AOP groups wrapped around the surface of the neighboring monomer while Pro2 and Phe0 in P2-RANTES are pointing different directions [Fig. 4(A,B)].

In the subunits A and B, P2-RANTES shows the N-termini to be clearly defined, and the extended Phe0 bound to the hydrophobic clefts of the subunit C and D, not interacting with its dimer partner. This is very different from the disordered amino terminus of native RANTES, and different from AOP-RANTES where the AOP group binds to the surface of the other subunit in the dimer.[68]

DISCUSSION

RANTES possesses the unique capacity to bind and activate a range of receptors including CCR1, CCR3, CCR4, and CCR5. To make a more potent anti-HIV entry inhibitor, Hartley et al. used phage display to both increase the affinity of a RANTES variant for CCR5 as well as increase selectivity, leading to the mutant P2-RANTES.[30] We show here that this unique chemokine mutant can be produced from *E. coli* and has an impressive HIV inhibitory capability. It is predominantly a monomer in solution, although it possesses the capacity to multimerize as shown in the crystal structure. Very recently, Gaertner et al.[31] used P2-RANTES as a starting point in a selection to find an even better set of RANTES derivatives in terms of anti-HIV potency.

The anti-HIV function of P2-RANTES expressed from *E. coli* (IC_{50} = 2.4 ± 0.8) was very similar to that of the chemically synthesized protein (IC_{50} = 0.6 – 1.6 n*M*).[31,30] Although it is possible that the *E. coli* version is slightly less potent, more likely the small difference in inhibitory IC_{50} is due to variations in assay conditions, which tend to vary slightly from lab to lab. Further, P2-RANTES showed selectivity for fusion inhibition in a cell–cell fusion assay in the presence of competing "unrelated" cells, while the peptide C37 does not. C37 shares a great deal of sequence with the clinically approved fusion inhibitor T-20, since both are derived from the sequence of the HIV protein gp41. In the absence of competing cells, P2-RANTES was ~18 fold better than C37 at inhibition, while in the presence of competing cells P2-RANTES was ~65 fold better than C37. This suggests that in a clinical setting P2-RANTES may be able to retain its high activity even in a complex physiological environment.

P2-RANTES is a pure monomer under most solution conditions, as judged by analytical ultracentrifugation [Fig. 2(B)], but the crystal structure reported in this study (crystallized at the same pH as the analytical ultracentrifugation) is a unique tetramer. This

difference in quaternary state could be because of the high concentration and unusual salt conditions used for crystal formation. Other chemokines have been observed to be monomers or dimers in solution while the crystal structures show higher order multimerization.[1,4,72] In the functional assays of P2-RANTES reported by Hartley, the authors specifically note that an aromatic residue in position zero is important.[30] Here, we report the structure of P2-RANTES, which also shows a structural role for Phe0 that indicates that Phe0 may be important in forming the unique tetramer structure. However, this structural importance may not reflect functional importance. In the recent next-generation RANTES mutants, this Phe0 is most often replaced with Gln.[31]

Although it is not clear exactly how the extended residue Phe0 in P2-RANTES interacts with CCR5, a comparison of the N-terminus of the structure that we report here to other available RANTES crystal structures shows that the Phe0 is oriented differently than Met0 in Met-RANTES or the AOP group in AOP-RANTES: Met0 is undefined in the crystal structure while the AOP group folds back to the surface of the other monomer.[34,68] Phe0 in P2-RANTES, however, points away from the dimer of subunit A and subunit B and binds to the hydrophobic cleft of subunit C in the tetramer. This may indicate a different function for Phe0 than the AOP group in an interaction with the receptor, although it could be an artifact of crystallization.

RANTES can form higher-order oligomers at high concentration[32] or in the presence of GAGs.[73] It has been shown in several studies that the GAG binding can alter the oligomerization of chemokines[40,62,66] and in particular can tighten the dimer. As shown in Results, P2-RANTES has diminished capacity to bind GAGs compared to the wild type protein [Fig. 2(A)]. This could be due to the weakened dimer in P2-RANTES, as mutations that comprise P2-RANTES such as Tyr3Leu, Asp6Gln, Thr7Ser, Thr8Ser, and Pro9Ala appear to reduce the intersubunit packing, possibly leading to the very weak dimer in P2-RANTES. The relation of the reduced GAG affinity for P2-RANTES and its potent increase in anti-HIV fusion activity compared to the wild type protein is not known.

In conclusion, we produced the previously reported potent anti-HIV-1 chemokine P2-RANTES from *E. coli* and found this unique protein to have significantly greater inhibitory potency than the widely used HIV fusion inhibitor, C37, particularly in the presence of competing "unrelated" cells. The crystal structure of P2-RANTES was determined at 1.7 Å resolution. Several intersubunit contact areas were identified in this tetramer crystal structure, although the protein was found to be a monomer under most solution conditions. This study provides both structural and functional details for this uniquely potent anti-HIV-1 chemokine. Further investigation of P2-RANTES will be of great value in the search for improved CCR5 receptor antagonists and will facilitate the development of agents to block HIV-1 entry.

ACKNOWLEDGMENTS

NMR experiments were carried out at the Biomolecular NMR Laboratory at Texas A&M University. The authors thank Dr. Lawrence Dangott and Sabrina Schmidtke from the Protein Chemistry Lab at Texas A&M University for the mass spectrum experiments. They also thank Dr. Xiangming Kong and Dr. Roger Smith for technical support, Dr. Jean-Philippe Pellois for offering the 3T3 cell line, and Jake Dennis for many useful discussions.

REFERENCES

1. Allen SJ, Crown SE, Handel TM. Chemokine: receptor structure, interactions, and antagonism. Annu Rev Immunol 2007;25:787–820.
2. Leonard JT, Roy K. The HIV entry inhibitors revisited. Curr Med Chem 2006;13:911–934.
3. Sheikine Y, Hansson GK. Chemokines and atherosclerosis. Ann Med 2004;36:98–118.
4. Fernandez EJ, Lolis E. Structure, function, and inhibition of chemokines. Annu Rev Pharmacol Toxicol 2002;42:469–499.
5. Gerard C, Rollins BJ. Chemokines and disease. Nat Immunol 2001; 2:108–115.
6. Wells TN, Proudfoot AE, Power CA. Chemokine receptors and their role in leukocyte activation. Immunol Lett 1999;65:35–40.
7. Alkhatib G, Combadiere C, Broder CC, Feng Y, Kennedy PE, Murphy PM, Berger EA. CC CKR5: a RANTES, MIP-1alpha, MIP-1beta receptor as a fusion cofactor for macrophage-tropic HIV-1. Science 1996; 272:1955–1958.
8. Alkhatib G, Locati M, Kennedy PE, Murphy PM, Berger EA. HIV-1 coreceptor activity of CCR5 and its inhibition by chemokines: independence from G protein signaling and importance of coreceptor downmodulation. Virology 1997;234:340–348.
9. Amzazi S, Ylisastigui L, Bakri Y, Rabehi L, Gattegno L, Parmentier M, Gluckman JC, Benjouad A. The inhibitory effect of RANTES on the infection of primary macrophages by R5 human immunodeficiency virus type-1 depends on the macrophage activation state. Virology 1998;252:96–105.
10. Vangelista L, Secchi M, Lusso P. Rational design of novel HIV-1 entry inhibitors by RANTES engineering. Vaccine 2008;26:3008–3015.
11. Longden J, Cooke EL, Hill SJ. Effect of CCR5 receptor antagonists on endocytosis of the human CCR5 receptor in CHO-K1 cells. Br J Pharmacol 2008;153:1513–1527.
12. Pakianathan DR, Kuta EG, Artis DR, Skelton NJ, Hebert CA. Distinct but overlapping epitopes for the interaction of a CC-chemokine with CCR1, CCR3 and CCR5. Biochemistry 1997; 36:9642–9648.
13. Ramnarine EJ, Devico AL, Vigil-Cruz SC. Analogues of N-terminal truncated synthetic peptide fragments derived from RANTES inhibit HIV-1 infectivity. Bioorg Med Chem Lett 2006; 16:93–95.
14. Nardese V, Longhi R, Polo S, Sironi F, Arcelloni C, Paroni R, Desantis C, Sarmientos P, Rizzi M, Bolognesi M, Pavone V, Lusso P. Structural determinants of CCR5 recognition and HIV-1 blockade in RANTES. Nat Str Biol 2001;8:611–615.
15. Struyf S, De Meester I, Scharpe S, Lenaerts JP, Menten P, Wang JM, Proost P, Van Damme J. Natural truncation of RANTES abolishes signaling through the CC chemokine receptors CCR1 and CCR3, impairs its chemotactic potency and generates a CC chemokine inhibitor. Eur J Immunol 1998;28:1262–1271.

16. Lim JK, Lu W, Hartley O, Devico AL. N-terminal proteolytic processing by cathepsin G converts RANTES/CCL5 and related analogs into a truncated 4–68 variant. J Leukocyte Biol 2006;80:1395–1404.
17. Ylisastigui L, Vizzavona J, Drakopoulou E, Paindavoine P, Calvo CF, Parmentier M, Gluckman JC, Vita C, Benjouad A. Synthetic full-length and truncated RANTES inhibit HIV-1 infection of primary macrophages. AIDS 1998;12:977–984.
18. Amara A, Gall SL, Schwartz O, Salamero J, Montes M, Loetscher P, Baggiolini M, Virelizier JL, Arenzana-Seisdedos F. HIV coreceptor downregulation as antiviral principle: SDF-1alpha-dependent internalization of the chemokine receptor CXCR4 contributes to inhibition of HIV replication. J Exp Med 1997;186:139–146.
19. Elsner J, Petering H, Hochstetter R, Kimmig D, Wells TN, Kapp A, Proudfoot AE. The CC chemokine antagonist Met-RANTES inhibits eosinophil effector functions through the chemokine receptors CCR1 and CCR3. Eur J Immunol 1997;27:2892–2898.
20. Elsner J, Petering H, Kimmig D, Wells TN, Proudfoot AE, Kapp A. The CC chemokine receptor antagonist met-RANTES inhibits eosinophil effector functions. Int Arch Allergy Immunol 1999;118: 462–465.
21. Grone HJ, Weber C, Weber KS, Grone EF, Rabelink T, Klier CM, Wells TN, Proudfood AE, Schlondorff D, Nelson PJ. Met-RANTES reduces vascular and tubular damage during acute renal transplant rejection: blocking monocyte arrest and recruitment. FASEB J 1999; 13:1371–1383.
22. Polo S, Nardese V, De Santis C, Arcelloni C, Paroni R, Sironi F, Verani A, Rizzi M, Bolognesi M, Lusso P. Enhancement of the HIV-1 inhibitory activity of RANTES by modification of the N-terminal region: dissociation from CCR5 activation. Eur J Immunol 2000;30: 3190–3198.
23. Proudfoot AE, Power CA, Hoogewerf AJ, Montjovent MO, Borlat F, Offord RE, Wells TN. Extension of recombinant human RANTES by the retention of the initiating methionine produces a potent antagonist. J Biol Chem 1996;271:2599–2603.
24. Proudfoot AE, Buser R, Borlat F, Alouani S, Soler D, Offord RE, Schroder JM, Power CA, Wells TN. Amino-terminally modified RANTES analogues demonstrate differential effects on RANTES receptors. J Biol Chem 1999;274:32478–32485.
25. Mack M, Luckow B, Nelson PJ, Cihak J, Simmons G, Clapham PR, Signoret N, Marsh M, Stangassinger M, Borlat F, Wells TN, Schlondorff D, Proudfoot AE. Aminooxypentane-RANTES induces CCR5 internalization but inhibits recycling: a novel inhibitory mechanism of HIV infectivity. J Exp Med 1998;187:1215–1224.
26. Sabbe R, Picchio GR, Pastore C, Chaloin O, Hartley O, Offord R, Mosier DE. Donor- and ligand-dependent differences in C-C chemokine receptor 5 reexpression. J Virol 2001;75:661–671.
27. Kawamura T, Bruse SE, Abraha A, Sugaya M, Hartley O, Offord RE, Arts EJ, Zimmerman PA, Blauvelt A. PSC-RANTES blocks R5 human immunodeficiency virus infection of Langerhans cells isolated from individuals with a variety of CCR5 diplotypes. J Virol 2004;78:7602–7609.
28. Hartley O, Gaertner H, Wilken J, Thompson D, Fish R, Ramos A, Pastore C, Dufour B, Cerini F, Melotti A, Heveker N, Picard L, Alizon M, Mosier D, Kent S, Offord R. Medicinal chemistry applied to a synthetic protein: development of highly potent HIV entry inhibitors. Proc Natl Acad Sci USA 2004;101:16460–16465.
29. Pastore C, Picchio GR, Galimi F, Fish R, Hartley O, Offord RE, Mosier DE. Two mechanisms for human immunodeficiency virus type 1 inhibition by N-terminal modifications of RANTES. Antimicrob Agents Chemother 2003;47:509–517.
30. Hartley O, Dorgham K, Perez-Bercoff D, Cerini F, Heimann A, Gaertner H, Offord RE, Pancino G, Debre P, Gorochov G. Human immunodeficiency virus type 1 entry inhibitors selected on living cells from a library of phage chemokines. J Virol 2003;77:6637–6644.
31. Gaertner H, Cerini F, Escola JM, Kuenzi G, Melotti A, Offord R, Rossitto-Borlat I, Nedellec R, Salkowitz J, Gorochov G, Mosier D, Hartley O. Highly potent, fully recombinant anti-HIV chemokines: reengineering a low-cost microbicide. Proc Natl Acad Sci USA 2008;105:17706–17711.
32. Skelton NJ, Aspiras F, Ogez J, Schall TJ. Proton NMR assignments and solution conformation of RANTES, a chemokine of the C-C type. Biochemistry 1995;34:5329–5342.
33. Chung C, Cooke RM, Proudfoot AEI, Wells TNC. The three-dimensional solution structure of RANTES. Biochemistry 1995;34: 3907–9314.
34. Hoover DM, Shaw J, Gryczynski Z, Proudfoot AEI, Wells T, Lubkowski J. The crystal structure of Met-RANTES: Comparison with native RANTES and AOP-RANTES. Protein Pept Lett 2000;7:73–82.
35. Hamburger AE, Kim S, Welch BD, Kay MS. Steric accessibility of the HIV-1 gp41 N-trimer region. J Biol Chem 2005;280:12567–12572.
36. Root MJ, Kay MS, Kim PS. Protein design of an HIV-1 entry inhibitor. Science 2001;291:884–888.
37. Pleskoff O, Treboute C, Brelot A, Heveker N, Seman M, Alizon M. Identification of a chemokine receptor encoded by human cytomegalovirus as a cofactor for HIV-1 entry. Science 1997;276:1874–1878.
38. Mkrtchyan SR, Markosyan RM, Eadon MT, Moore JP, Melikyan GB, Cohen FS. Ternary complex formation of human immunodeficiency virus type 1 Env, CD4, and chemokine receptor captured as an intermediate of membrane fusion. J Virol 2005;79:11161–11169.
39. Wei X, Decker JM, Liu H, Zhang Z, Arani RB, Kilby JM, Saag MS, Wu X, Shaw GM, Kappes JC. Emergence of resistant human immunodeficiency virus type 1 in patients receiving fusion inhibitor (T-20) monotherapy. Antimicrob Agents Chemother 2002;46:1896–1905.
40. McCornack MA, Boren DM, LiWang PJ. Glycosaminoglycan disaccharide alters the dimer dissociation constant of the chemokine MIP-1 beta. Biochemistry 2004;43:10090–10101.
41. Pace CN, Vajdos F, Fee L, Grimsley G, Gray T. How to measure and predict the molar absorption coefficient of a protein. Protein Sci 1995;4:2411–2423.
42. Potterton L, Mcnicholas S, Krissinel E, Gruber J, Cowtan K, Emsley P, Murshudov GN, Cohen S, Perrakis A, Noble M. Developments in the CCP4 molecular-graphics project. Acta Crystallogr D-Biol Crystallogr 2004;60:2288–2294.
43. Brunger AT, Adams PD, Clore GM, Delano WL, Gros P, Grosse-Kunstleve RW, Jiang JS, Kuszewski J, Nilges M, Pannu NS, Read RJ, Rice LM, Simonson T, Warren GL. Crystallography & NMR system: A new software suite for macromolecular structure determination. Acta Crystallogr D-Biol Crystallogr 1998;54:905–921.
44. Demeler B, Saber H, Hansen JC. Identification and interpretation of complexity in sedimentation velocity boundaries. Biophys J 1997; 72:397–407.
45. Van Holde KE. WOW. Boundary analysis of sedimentation-velocity experiments with monodisperse and paucidisperse solutes. Biopolymers 1978;17:1387–1403.
46. Wishart DS, Bigam CG, Yao J, Abildgaard F, Dyson HJ, Oldfield E, Markley JL, Sykes BD. ^{1}H, ^{13}C, ^{15}N chemical shift referencing in biomolecular NMR. J Biomol NMR 1995;6:135–140.
47. Delaglio F, Grzesiek S, Vuister GW, Hu G, Pfeifer J, Bax A. NMRPipe: A multidimensional spectral processing system based on UNIX pipes. J Biomol NMR 1995;6:277–293.
48. Garrett DS, Powers R, Gronenborn AM, Clore GM. A common sense approach to peak picking in two-, three-, and four-dimensional spectra using automatic computer analysis of contour diagrams. J Magn Reson 1991;95:214–220.
49. Delean A, Munson PJ, Rodbard D. Simultaneous analysis of families of sigmoidal curves: application to bioassay, radioligand assay, and physiological dose-response curves. [see comment]. Am J Physiol 1978;235:E97–102.
50. Cheng-Mayer C, Liu R, Landau NR, Stamatatos L. Macrophage tropism of human immunodeficiency virus type 1 and utilization of the CC-CKR5 coreceptor. J Virol 1997;71:1657–1661.

51. Jin H, Shen X, Baggett BR, Kong X, LiWang PJ. The human CC chemokine MIP-1beta dimer is not competent to bind to the CCR5 receptor. J Biol Chem 2007;282:27976–27983.
52. Liu S, Lu H, Niu J, Xu Y, Wu S, Jiang S. Different from the HIV fusion inhibitor C34, the anti-HIV drug Fuzeon (T-20) inhibits HIV-1 entry by targeting multiple sites in gp41 and gp120. J Biol Chem 2005;280:11259–11273.
53. Veiga AS, Santos NC, Loura LM, Fedorov A, Castanho MA. HIV fusion inhibitor peptide T-1249 is able to insert or adsorb to lipidic bilayers. Putative correlation with improved efficiency. J Am Chem Soc 2004;126:14758–14763.
54. Root MJ, Steger HK. HIV-1 gp41 as a target for viral entry inhibition. Curr Pharm Des 2004;10:1805–1825.
55. Barretina J, Blanco J, Armand-Ugon M, Gutierrez A, Clotet B, Este JA. Anti-HIV-1 activity of enfuvirtide (T-20) by inhibition of bystander cell death. Antiviral Therapy 2003;8:155–161.
56. Le Y, Zhou Y, Iribarren P, Wang J. Chemokines and chemokine receptors: their manifold roles in homeostasis and disease. Cell Mol Immunol 2004;1:95–104.
57. Laing KJ, Secombes CJ. Chemokines. Dev Comp Immunol 2004;28: 443–460.
58. Lau EK, Allen S, Hsu AR, Handel TM. Chemokine-receptor interactions: GPCRs, glycosaminoglycans and viral chemokine binding proteins. Adv Protein Chem 2004;68:351–391.
59. Proudfoot AEI, Fritchley S, Borlat F, Shaw JP, Vilbois F, Zwahlen C, Trkola A, Marchant D, Clapham PR, Wells TNC. THe BBXB motif of RANTES is the principal site for heparin binding and controls receptor selectivity. J Biol Chem 2001;276:10620–10626.
60. Shaw JP, Johnson Z, Borlat F, Zwahlen C, Kungl A, Roulin K, Harrenga A, Wells TN, Proudfoot AE. The X-ray structure of RANTES: heparin-derived disaccharides allows the rational design of chemokine inhibitors. Structure 2004;12:2081–2093.
61. Mccornack MA, Cassidy CK, Liwang PJ. The binding surface and affinity of monomeric and dimeric chemokine MIP-1β for various glycosaminoglycan disaccharides. J Biol Chem 2003;278:1946–1956.
62. Proudfoot AE, Handel TM, Johnson Z, Lau EK, LiWang P, Clark-Lewis I, Borlat F, Wells TN, Kosco-Vilbois MH. Glycosaminoglycan binding and oligomerization are essential for the in vivo activity of certain chemokines. Proc Natl Acad Sci USA 2003;100:1885–1890.
63. Martin L, Blanpain C, Garnier P, Wittamer V, Parmentier M, Vita C. Structural and functional analysis of the RANTES-glycosaminoglycans interactions. Biochemistry 2001;40:6303–6318.
64. Laurence JS, LiWang AC, LiWang PJ. Effect of N-terminal truncation and solution conditions on chemokine dimer stability: nuclear magnetic resonance structural analysis of macrophage inflammatory protein 1β Mutants. Biochemistry 1998;37:9346–9354.
65. Kuloglu ES, Mccaslin DR, Markley JL, Volkman BF. Structural rearrangement of human lymphotactin, a C chemokine, under physiological solution conditions. J Biol Chem 2002;277:17863–17870.
66. Veldkamp CT, Peterson FC, Pelzek AJ, Volkman BF. The monomer-dimer equilibrium of stromal cell-derived factor-1 (CXCL 12) is altered by pH, phosphate, sulfate, and heparin. Protein Sci 2005;14: 1071–1081.
67. Pettersen EF, Goddard TD, Huang CC, Couch GS, Greenblatt DM, Meng EC, Ferrin TE. UCSF Chimera--a visualization system for exploratory research and analysis. J Comput Chem 2004;25:1605–1612.
68. Wilken J, Hoover D, Thompson DA, Barlow PN, Mcsparron H, Picard L, Wlodawer A, Lubkowski J, Kent SB. Total chemical synthesis and high-resolution crystal structure of the potent anti-HIV protein AOP-RANTES. Chem Biol 1999;6:43–51.
69. Mellado M, Rodriguez-Frade JM, Manes S, Martinez AC. Chemokine signaling and functional responses: the role of receptor dimerization and TK pathway activation. Annu Rev Immunol 2001;19: 397–421.
70. Clark-Lewis I, Kim K-S, Rajarathnam K, Gong J-H, Dewald B, Moser B, Baggiolini M, Sykes BD. Structure-activity relationships of chemokines. J Leukoc Biol 1995;57:703–711.
71. Hoover DM, Mizoue LS, Handel TM, Lubkowski J. The crystal structure of the chemokine domain of fractalkine shows a novel quaternary arrangement. J Biol Chem 2000;275:23187–23193.
72. Lubkowski J, Bujacz G, Boque L, Domaille PJ, Handel TM, Wlodawer A. The structure of MCP-1 in two crystal forms provides a rare example of variable quaternary interactions. Nat Struct Biol 1997;4:64–69.
73. Hoogewerf AJ, Kuschert GSV, Proudfoot AEI, Borlat F, Clark-Lewis I, Power CA, Wells TNC. Glycosaminoglycans mediate cell surface oligomerization of chemokines. Biochemistry 1997;36:13570–13578.